buildings

MDPI

Article

Computational Assessment of the Thermoenergetic Performance of an Earth-Air Heat Exchanger in Social Housing in Brazilian Bioclimatic Zones

Paula Wrague Moura [1], Márcio Wrague Moura [1], Luiz Alberto Oliveira Rocha [1], Elizaldo Domingues dos Santos [1], Ruth da Silva Brum [2] and Liércio André Isoldi [1,*]

[1] School of Engineering, Federal University of Rio Grande—FURG, Rio Grande 96203-900, RS, Brazil; pwmoura@gmail.com (P.W.M.); mwmoura@gmail.com (M.W.M.); luizrocha@furg.br (L.A.O.R.); elizaldosantos@furg.br (E.D.d.S.)

[2] Engineering Center, Federal University of Pelotas—UFPel, Pelotas 96010-020, RS, Brazil; ruthdasilvabrum@gmail.com

* Correspondence: liercioisoldi@furg.br

Abstract

Earth–Air Heat Exchangers (EAHEs) are passive systems that use the thermal interaction between air and soil along buried ducts to moderate supply air temperature, thereby lowering building energy consumption and improving indoor comfort conditions. This device has been employed in several countries and under diverse climatic characteristics. The integration of EAHE systems with bioclimatic design strategies contributes to improved building energy performance and more efficient use of thermal resources. This study aims to computationally investigate the thermoenergetic performance of EAHE system, for both cooling and heating purposes, installed in Social Housing (SH) across different Brazilian bioclimatic zones, and to propose strategies that improve the energy efficiency of these built environments. The study involves the validation and verification of a computational model and the thermoenergetic assessments of an SH unit, investigating different solar orientations and the installation of EAHE. These evaluations are performed via dynamic simulations conducted with the EnergyPlus software. The results show that the installation of the EAHE system coupled to the SH improves the thermoenergetic performance of the indoor environment, mainly by enhancing thermal comfort across different Brazilian bioclimatic zones (BZ). In BZ2R, the EAHE increased the annual *PHFT* by 4.5%, corresponding to seventeen additional days per year within the acceptable operative temperature range. The highest monthly improvement was observed in BZ1M, where the *PHFT* increased by 14.3% in January, equivalent to more than four additional days of thermal comfort in that month. The system proved to be more effective in zones 1M, 2R, 3B, and 4B, particularly in climates with lower annual average dry-bulb temperatures. Regarding energy performance, the EAHE showed benefits in specific months and conditions, indicating that its feasibility should be assessed through monthly thermoenergetic analyses rather than only annual indicators. This work provides validated and verified references and parameters for future projects and contributes to the state of the art in this field, as there are still few studies evaluating EAHE systems integrated into buildings using this software, despite its widespread use in building performance analysis.

Keywords: numerical simulation; computational modeling; energy efficiency; EnergyPlus

Check for updates

Academic Editors: Kai Zhang, Junming Zhou, Zhaofeng Dai and Weixue Jiang

Received: 16 April 2026
Revised: 3 June 2026
Accepted: 3 June 2026
Published: 5 June 2026

1. Introduction

According to the *Statistical Review of World Energy* by British Petroleum [1], more than 84% of the world's primary energy consumption was generated from fossil fuels (oil, natural gas, and coal). The available energy sources are limited, and their use leads to environmental issues such as global warming and air pollution [2].

Buildings account for over 30% of total global energy consumption [3,4], with approximately 72% attributed to the residential sector [5]. In Brazil, following the global trend, the residential sector shows the highest energy consumption among buildings, accounting for 10.9% of primary energy and 26.4% of electricity consumption, the highest share within the building sector [6]. A significant portion of this energy is consumed to maintain indoor thermal comfort through air conditioning or heating systems [7]. Furthermore, in recent decades, electricity consumption by air conditioning systems in buildings has been steadily increasing worldwide [8].

In recent years, research and development activities in residential heating and cooling technologies have increased, as approximately 16% of the world's total energy is consumed in the residential and commercial sectors for this purpose [9].

Thus, energy consumption in buildings for heating and cooling continues to rise year after year to meet the growing demand for thermal comfort. As a key energy issue in the construction sector, the largest energy consumer, there is a pressing need for the rational use of traditional resources and the adoption of clean and inexhaustible renewable energy technologies that enable sustainable development [10].

Due to the energy and environmental impacts associated with conventional heating and cooling systems, several renewable-energy-based and passive technologies have been studied and implemented worldwide to reduce energy consumption and improve thermal comfort in buildings [11]. In this context, ground thermal energy is a renewable resource that can be used for space conditioning (heating and cooling) and electricity savings through the use of Earth-Air Heat Exchangers (EAHE) in built environments. An EAHE is a passive thermal conditioning system in which air is forced to flow through buried ducts, exchanging heat with the surrounding soil and thereby being heated or cooled depending on the thermal conditions. This exchange occurs due to the ground's thermal inertia, meaning that in the summer, the air exiting the EAHE has a lower temperature than the outside air, while in the winter, the outdoor air is warmed as it flows through the EAHE and exits at a higher temperature [12].

Therefore, the EAHE is an energy-efficient technology that can help reduce energy consumption in buildings without carbon dioxide emissions or any environmental impact [13]. The system's heating and cooling capacity is closely tied to the thermal variability of its location, making climate a critical factor for the proper functioning of the system [14].

According to recent studies [10,12,15–21] conducted in countries such as Canada, Brazil, the United Arab Emirates, Italy, France, China, and Algeria, the results demonstrated that the EAHE can be used as a pre-conditioning system to heat air during cold periods and cool it during hot periods. Thus, the EAHE showed good thermo-energetic performance under different climatic conditions, improving thermal comfort and saving energy in all the regions investigated.

In addition to climate, other relevant factors influence the efficiency of the EAHE system, including soil type, duct depth and length, and airflow velocity. EAHE systems installed in soils with clayey layers showed superior thermal performance compared to those installed in predominantly sandy soils, although the heating and cooling potential of the EAHE does not necessarily increase with greater installation depth [22]. Similarly, an energy and economic comparison between silt and quartzite showed that silt generally provides higher efficiency [23]. The length of the EAHE also significantly affects its outlet

https://doi.org/10.3390/buildings16112285

air temperature [24], while pipe radius, length, and depth, as well as airflow velocity and soil characteristics, have been identified as the most impactful parameters affecting EAHE performance [15].

Therefore, the use of shallow geothermal energy for direct improvement of indoor thermal conditions has shown positive results, contributing to thermal performance while reducing energy consumption and pollutant emissions from buildings.

It is also important to highlight the relevance of integrating this technology with bioclimatic strategies and energy efficiency measures, as their combined application enhances the performance of buildings as integrated systems. The efficiency and usefulness of the EAHE system can be improved when combined with other technologies [25].

Another relevant aspect is the relatively low construction and operational cost of EAHE systems compared to conventional air conditioners [26,27], making it a viable alternative for low-income housing.

A major challenge in Brazil is the limited access to housing for a substantial portion of the population, especially among low-income families. According to recent estimates [28], based on data from the Continuous National Household Sample Survey (PnadC) by the Brazilian Institute of Geography and Statistics (IBGE) and the Unified Registry for Social Programs, the estimated housing deficit in 2022 was 6,215,313 housing units, representing 8.3% of all occupied dwellings in the country.

To address this housing deficit, the Federal Government launched the *Minha Casa, Minha Vida* Program (PMCMV) in 2009 [29], followed by the *Casa Verde e Amarela* Program in 2021 [30], and has recently resumed the PMCMV in an effort to facilitate home ownership for low-income families. These government programs contribute to reducing Brazil's housing shortage. However, their replicable designs often disregard the adequacy of building layout and envelope for local climatic conditions [31].

In this context, aiming to accelerate the construction process and reduce costs, Social Housing (SH) projects have been developed as standardized models nationwide, without considering regional specificities, climatic conditions, or construction materials [4,32]. This approach results in buildings that do not adequately respond to the local climate, making the use of artificial air conditioning systems necessary and, consequently, increasing electricity consumption.

Furthermore, it is important to note that Brazil has a highly diverse climate due to its vast territory and its location between the two tropics. The different Brazilian climates are classified according to NBR 15220 [33], which defines the Brazilian bioclimatic zoning system, composed of six bioclimatic zones gradually ranging from "very cold" to "very hot." The cold zones are subdivided according to the heating thermal load, while the other bioclimatic zones are subdivided based on relative humidity, resulting in twelve zones. The present study covers six zones from the updated standard, whereas the previous standard included all bioclimatic zones.

Although previous studies, including recent works published between 2023 and 2026 [3,14,18,19,23], have advanced the analysis of EAHE systems by investigating climatic effects, soil properties, duct configurations, optimization procedures, and coupling strategies with building energy systems, most of them have focused on isolated EAHE configurations, specific climatic regions, or limited sets of design parameters. Therefore, there is still a lack of studies that combine a verified and validated dynamic simulation framework in EnergyPlus with the assessment of an EAHE system integrated into a standardized SH unit across representative Brazilian bioclimatic zones. Unlike previous studies, the present work simultaneously considers solar orientation, local soil characteristics, annual and monthly thermoenergetic indicators, and the thermal performance criteria established by Brazilian standards. This broader approach allows the identification of the bioclimatic conditions under which the EAHE is more suitable for SH and supports the development of more climate-responsive design strategies.

Based on these considerations, the following research questions arise, which this study seeks to answer:

(I) Do SH units present adequate thermoenergetic performance for their intended use, even when using a standardized design across different regions of Brazil?
(II) Is the EAHE system effective in improving the thermoenergetic conditions of SH in different Bioclimatic Zones (BZs)?
(III) Which bioclimatic improvement strategies result in more thermoenergetically efficient buildings?

In this context, the main goal of this study is to computationally evaluate the thermoenergetic performance of an EAHE system, for both cooling and heating, integrated into a SH unit across different Brazilian BZs, and to propose strategies aimed at improving the energy efficiency in this type of built environment.

2. Materials and Methods

To perform the proposed investigation, in addition to the literature review presented previously, the following methodological steps are adopted:

(I) Verification and validation of the computational model in EnergyPlus;
(II) Determination of a building model for case study analysis;
(III) Definition of the simulation cases;
(IV) Analysis of the soil characteristics of each BZ and the characteristics of the EAHE system;
(V) Evaluation of the thermoenergetic performance of the SH unit in each BZ;
(VI) Evaluation of the thermoenergetic performance of the SH with the EAHE system installed in each BZ;
(VII) Comparative assessment of the defined scenarios, aiming at improving the thermoenergetic performance of the SH.

To improve the clarity of the solution method, Figure 1 summarizes the methodological workflow adopted in the computational assessment, from model verification and validation to the definition of input data, simulation scenarios, performance indicators, and comparative analysis.

As shown in Figure 1, the computational procedure was organized into two main simulation stages. First, the reference and actual SH models were evaluated across the representative Brazilian BZs and solar orientations. Then, based on the best and worst solar-orientation results, the EAHE system was coupled to the actual SH model to assess its effect on the thermoenergetic performance indicators.

2.1. Verification and Validation of the Computational Model

For the verification and validation of the computational model, the Casa Ventura building (Figure 2), located in the city of Viamão—RS, is used [34,35].

The thermal behavior is evaluated, and the obtained results are compared with the numerical study reported in [36] for verification and with the experimental data presented in [34,35] for validation, following the methodology described in [37].

2.2. Determination of a Building Model

The selected building model corresponds to a single-family SH typology based on the standardized design guidelines provided by CAIXA (Standard Project—*Casas Populares*) [38], within the scope of the *Minha Casa, Minha Vida* (PMCMV) program [39]. This particular model was chosen due to the availability of detailed construction specifications and technical information, as well as the use of commonly adopted low-cost building materials typical of SH developments.

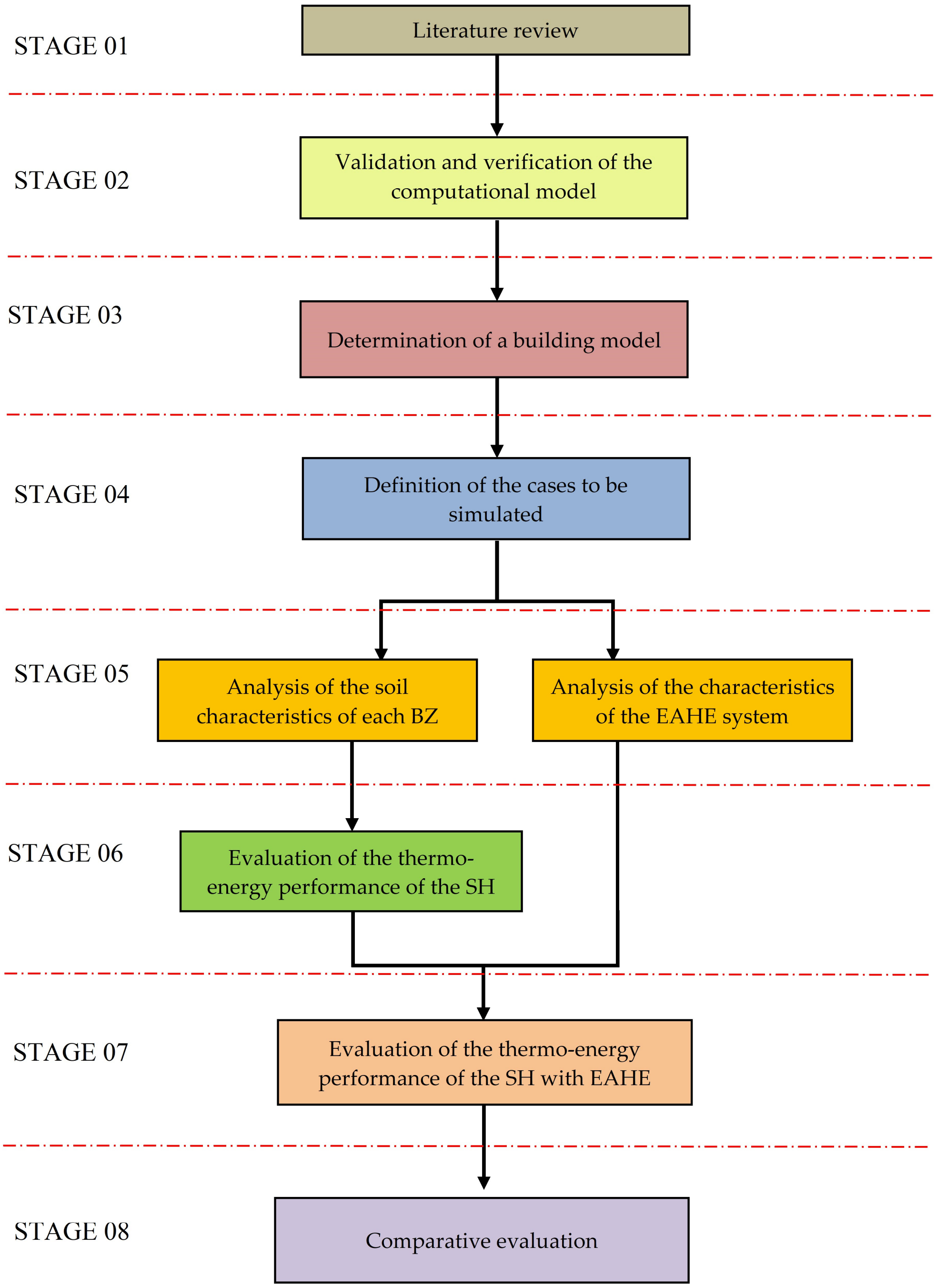

Figure 1. Schematic representation of the methodological workflow.

The model presents a total built area of 41.87 m^2, comprising a living room integrated with the kitchen, two bedrooms, and a bathroom, as illustrated in Figures 3 and 4. All walls are constructed using ceramic masonry with six-hole bricks measuring 20 × 15 × 10 cm. The exterior surfaces are finished with roughcast and plaster, while the interior surfaces consist of exposed brickwork, except in the bathroom and kitchen areas. The roofing system is composed of 5 mm thick fiber cement tiles with a 15° slope, and all interior spaces are finished with polyvinyl chloride (PVC) ceilings. The flooring consists of cement-based material, and the window and door frames are made of wood and single-pane 3 mm glass.

(**a**) (**b**)

Figure 2. Casa Ventura building: (**a**) façade and (**b**) floor plan.

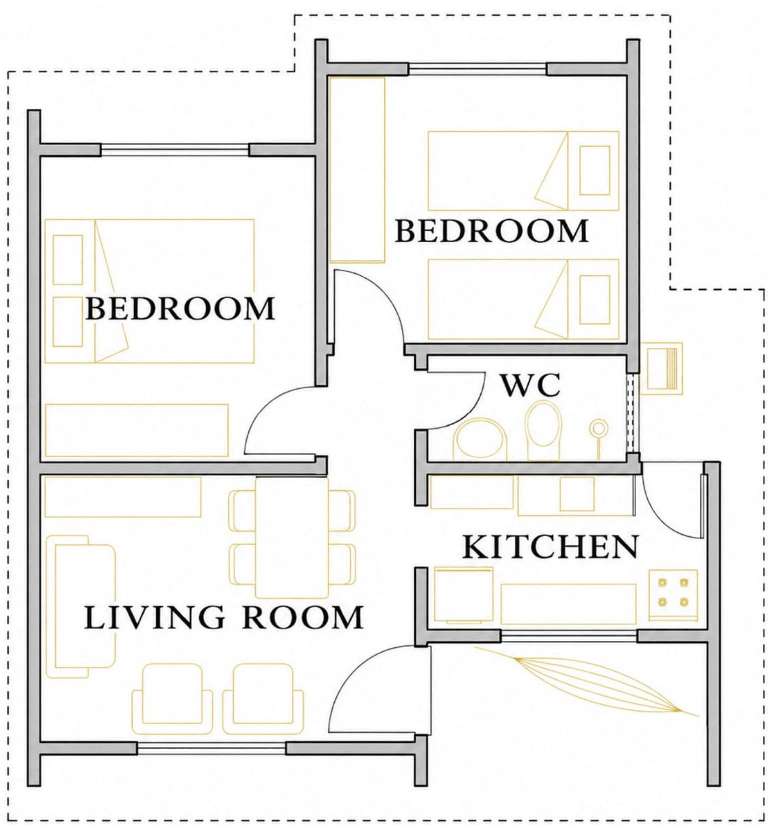

Figure 3. Floor plan of the SH.

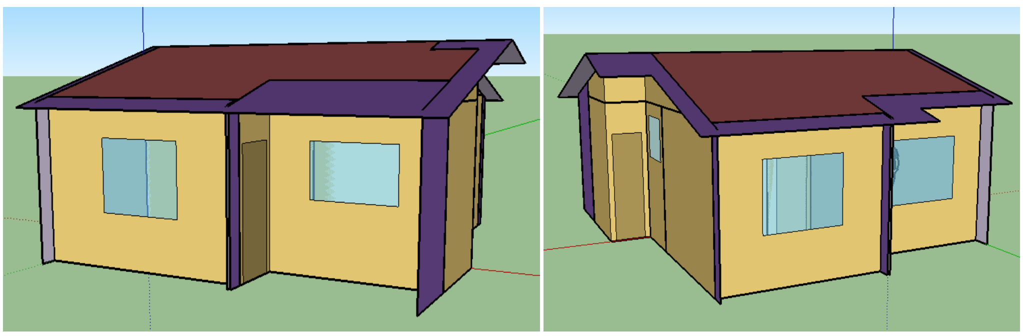

(**a**) (**b**)

Figure 4. Computationally modeled volumetry of the SH: (**a**) perspective view of the living room and kitchen façade; (**b**) perspective view of the bedroom façade.

2.3. Description of the Simulation Scenarios

The following simulation scenarios were defined based on the considered SH model:

(I) Scenario 1: SH model in the six representative cities, using weather files and considering the highest percentage of openings oriented toward each solar direction (north (N), northeast (NE), east (E), southeast (SE), south (S), southwest (SW), west (W), and northwest (NW)), in accordance with the computational simulation procedure of NBR 15575 [40]. The simulations include the reference model and the actual SH model, both with and without natural ventilation. Therefore, for each representative city, 32 cases are simulated. As there are six cities, Scenario 1 results in a total of 192 simulated cases.

(II) Scenario 2: from the perspective of thermoenergetic performance, simulations focused on two indicators: *PHFT* (Percentage of Occupied Hours within an Operative Temperature Range), considering natural ventilation, and CgTT (Total Thermal Load), without natural ventilation. The best and worst-performing results from Scenario 1, in terms of solar orientation, were analyzed using the EAHE system across the six representative cities, resulting in 8 cases per city, and thus 48 cases in total for Scenario 2.

Combining both scenarios, a total of 240 simulation cases were analyzed. To improve the clarity and reproducibility of the simulation procedure, the main input data and evaluated conditions for each simulation scenario are summarized in Table 1.

Table 1. Summary of the simulation scenarios and main input data.

Scenario	Model Evaluated	Main Input Data	Evaluated Conditions	Performance Indicators	Number of Cases
1	Reference model and actual SH model	Six representative Brazilian bioclimatic zones; TRY weather files; eight solar orientations; building envelope properties; natural ventilation condition	Actual and reference models, with and without natural ventilation, considering N, NE, E, SE, S, SW, W, and NW orientations	*PHFT* and *CgTT*	192
2	Actual SH model coupled to the EAHE	Best and worst solar orientations obtained from Scenario 1; EAHE geometry and operating parameters; soil properties; weather files of the representative cities	Actual SH model with and without EAHE, considering the best and worst solar orientations for each representative bioclimatic zone	*PHFT* and *CgTT*	48
Total	—	—	Combination of Scenarios 1 and 2	*PHFT* and *CgTT*	240

2.4. Analysis of Soil Characteristics in Each BZ

The soil characteristics were analyzed using Standard Penetration Tests (SPT) to obtain information regarding soil type and groundwater level. The thermophysical properties of the soils, such as bulk density, specific heat capacity, thermal conductivity, and characteristic temperatures were adopted from [41,42]. These values can be found in Table 2. Specifically for BZ2R, the soil properties, including soil type and groundwater level, were also defined based on [34,35].

Table 2. Soil Data for the studied BZs.

BZ	Representative City	Thermal Properties of Soil [41]			EnergyPlus (CalcSoilSurfTemp)		
		Conductivity (W/m·K)	Specific Mass (kg/m^3)	Specific Heat (J/kg·K)	Average Annual Ground Surface Temperature	Ground Surface Temperature Range	Phase Constant of Soil Surface Temperature
1M	CURITIBA—PR	1.58	2000	1550	18.61883163	3.970953703	196
2R	VIAMÃO—RS	2.1	1800	1780	21.37354088	6.56166744	216
3B	BRASÍLIA—DF	1.58	2000	1550	24.25137711	1.32330024	237

Table 2. *Cont.*

BZ	Representative City	Thermal Properties of Soil [41]			EnergyPlus (CalcSoilSurfTemp)		
		Conductivity (W/m·K)	Specific Mass (kg/m^3)	Specific Heat (J/kg·K)	Average Annual Ground Surface Temperature	Ground Surface Temperature Range	Phase Constant of Soil Surface Temperature
4B	GOIÂNIA—GO	0.25	1600	890	26.14668465	10.20217800	102
5B	CUIABÁ—MT	0.25	1600	890	28.27702522	14.12667847	206
5A	RECIFE—PE	0.25	1600	890	27.27695656	4.00676012	190

2.5. Analysis of the Characteristics of the EAHE System

The characteristics of the EAHE system were obtained from [34,35], considering a duct with a diameter of 110 mm and a length of 34 m, made of PVC material, installed at a depth of 3 m, and with an airflow velocity inside the duct of 3.3 m/s. Additionally, grass is assumed as the ground surface cover since previous studies [16,24,43] indicate that it enhances the thermal performance of the EAHE system, reducing the need for deep duct installation and facilitating maintenance.

For this study, a straight duct was considered installed for each Prolonged Occupancy Area (APP) of the SH, i.e., in the living room-kitchen and the two bedrooms.

2.6. Evaluation of the Thermoenergetic Performance of the SH in Each BZ

For the evaluation of the thermoenergetic performance of the SH, the computational simulation procedure established by NBR 15575 [40], which pertains to the performance of residential buildings, was adopted.

This computational simulation procedure assesses the annual thermal performance of the building envelope in relation to a reference envelope. Two models must be developed in this procedure:

(I) The real model, which preserves the geometric characteristics of the SH, as well as the thermal properties and compositions of the transparent elements, walls, and roof;
(II) The reference model, which represents the evaluated building but with reference characteristics, as detailed in Table 3.

The real and reference models are simulated with the use of natural ventilation in the APP to assess compliance with the minimum level of thermal performance. Simulations are also carried out without natural ventilation to evaluate whether the intermediate and superior levels of thermal performance are achieved.

Based on the simulation considering the use of natural ventilation, the following indicators are determined:

(I) The percentage of occupied hours within the operative temperature range in the Prolonged Occupancy Areas (*PHFTAPP*);
(II) The annual maximum (*TomaxAPP*) and minimum (*TominAPP*) operative temperatures of each APP, considering only the occupancy periods of each APP.

From the simulation without the use of natural ventilation, the following indicators are determined:

(I) The annual sum of the hourly cooling thermal load values (*CgTRAPP*);
(II) The annual sum of the hourly heating thermal load values (*CgTAAPP*).

Based on the *CgTRAPP* and *CgTAAPP* values for each APP, the annual sum of the hourly total thermal load of the housing unit (*CgTTUH*) is calculated.

The cooling thermal load is calculated using a setpoint temperature of 23 °C, with activation only during the periods in which the APP is occupied. The same idealized thermal load calculation system is applied for heating, using a heating setpoint temperature of 21 °C, also triggered only during the occupancy periods of each APP.

Table 3. Characteristics of the reference model and the real model.

Parameters Analyzed								
Reference model								
			Conductivity W/(m·K)	Specific heat J/(kg·K)	Absorbance	Emissivity	Density (kg/m^3)	Transmittance W/(m^2·K)
Floors			1.75	1000	0.70	0.90	2200	
Walls	External		1.75	1000	0.58	0.90	2200	4.40
	Internal		1.75	1000	0.20	0.90	2200	
Roof	Roof tile 6 mm		0.65	840	0.65	0.90	1700	2.06
		Air chamber	Thermal resistance ((m^2·K)/K) = 0.21					
	Slab 100 mm		1.75	1000	0.70	0.90	2200	
			Thermal resistance (m^2·K)/K		Absorbance	Emissivity		
	BZ 5A	Thermal insulation	0.67		0.70	0.90		
Real model								
			Conductivity W/(m·K)	Specific heat J/(kg·K)	Absorbance	Emissivity	Density (kg/m^3)	Transmittance W/(m^2·K)
Floors		Cemented 20 mm Radiator 100 mm	1.75	1000	0.70	0.90	2200	
Walls	External	Ceramic brick 6 holes	0.90	920	0.20	0.90	1600	2.82
		Air chamber	Thermal resistance ((m^2·K)/W) = 0.0961					
		Ceramic brick 6 holes	0.90	920	0.20	0.90	1600	
		Mortar	1.15	1000	0.20	0.90	2000	
	Internal	Ceramic brick 6 holes	0.90	920	0.20	0.90	1600	
		Air chamber	Thermal resistance ((m^2·K)/W) = 0.0961					
		Ceramic brick 6 holes	0.90	920	0.20	0.90	1600	
Roof		Fiber cement tile	0.95	840	0.57	0.90	1900	1.76
		Air chamber	Thermal resistance ((m^2·K)/W) = 0.21					
		PVC lining	0.071	960	0.20	273		

In the building modeling, internal loads are considered through user occupancy in the APP, as well as the use of artificial lighting and equipment, in accordance with NBR 15575 [40].

Development of the Numerical Model

The computational domain of the building was developed using the graphical interface of SketchUp 2017 software, with the Euclid plugin, where the thermal zones were defined based on the building geometry and boundary conditions. The thermoenergetic computational simulations were performed using EnergyPlus software, version 9.4, which adopts a heat balance-based formulation to calculate the transient thermal behavior of building zones. In this approach, the thermal response of the building envelope is determined by considering conduction through opaque elements, convection at internal and external surfaces, long-wave radiation exchange, and the absorption and transmission of short-wave solar radiation. Solar gains are calculated from the direct normal and diffuse horizontal solar radiation data provided by the weather file, considering the solar position, surface orientation, tilt angle, shading effects, and the optical properties of transparent and opaque envelope components. Therefore, the incident solar radiation on each external surface is obtained as a function of the local climatic conditions and the geometric configuration of the building.

For the indoor thermal analysis, EnergyPlus solves the zone air heat balance by accounting for internal gains, heat exchange with the envelope, infiltration, ventilation, and interzone airflows, when applicable. Natural ventilation was represented according to the defined opening schedules and airflow conditions, allowing the assessment of its influence on indoor thermal performance. The ground thermal boundary condition was defined using the soil temperature data adopted in the simulations, which directly affects the heat exchange between the buried ducts of the EAHE and the surrounding soil. The EAHE was modeled as an earth tube system, in which outdoor air flows through buried ducts before entering the building zone, enabling heat exchange with the soil and modifying the inlet air temperature supplied to the indoor environment.

Thus, the numerical model accounts for the coupled influence of climate, solar orientation, building envelope properties, natural ventilation, and soil–air heat exchange on the thermal performance of the social housing model. This modeling strategy allows the comparison between the reference case and the EAHE-assisted case under different Brazilian bioclimatic conditions.

The EnergyPlus software calculates the energy balance for each Thermal Zone (TZ) using the predictor-corrector method, which employs an explicit scheme to estimate the next iteration result, followed by an implicit scheme to recalculate this value, progressively approximating the real value [42], using:

$$C_Z \frac{dT_Z}{dt} = \sum_{i=1}^{N_{sl}} \dot{Q}_i + \sum_{i=1}^{N_{\text{surface}}} h_i A_i (T_{si} - T_{ext}) + \sum_{i=1}^{N_{zones}} \dot{m}_i C_p (T_{si} - T_{ext}) + m_{inf} C_p (T_\infty - T_{ext}) + \dot{Q}_{sys} \quad (1)$$

where $\sum_{i=1}^{N_{sl}} \dot{Q}_i$ is the sum of internal convective loads; $\sum_{i=1}^{N_{\text{surface}}} h_i A_i (T_{si} - T_{ext})$ is the convective heat transfer through the zone surfaces; T_{ext} is the external temperature; $m_{inf} C_p (T_\infty - T_{ext})$ is the heat transfer due to outdoor air infiltration; $\sum_{i=1}^{N_{zones}} \dot{m}_i C_p (T_{si} - T_{ext})$ is the heat transfer due to interzone air mixing; $\dot{Q}_{sys}$ is the heat supplied or removed by the air system; and $C_Z \frac{dT_Z}{dt}$ is the rate of energy stored in the thermal zone. The subscript i denotes the i-th surface or the i-th zone.

For the heat flux calculated on the surfaces, convective, conductive, and radiative exchanges must be considered. For external walls, the following applies [42]:

$$q''_{\alpha sol} + q''_{LWR} + q''_{conv} - q''_{ko} = 0 \quad (2)$$

where $q''_{\alpha sol}$ is the radiative heat flux absorbed from direct and diffuse solar radiation; q''_{LWR} is the longwave radiation flux exchanged with the air and surroundings; q''_{conv} is the convective heat flux; and q''_{ko} is the conductive heat flux into the interior of the wall.

For internal walls, the following applies [42]:

$$q''_{LWX} + q''_{ki} + q''_{SW} + q''_{LWS} + q''_{sol} + q''_{conv} = 0 \quad (3)$$

where q''_{LWX} is the longwave radiative heat flux between thermal zone surfaces; q''_{ki} is the conductive heat flux through the wall; q''_{SW} is the shortwave radiative heat flux between thermal zone surfaces; q''_{LWS} is the longwave radiative flux from the zone equipment; q''_{sol} is the solar radiation heat flux absorbed by the surface; and q''_{conv} is the convective heat flux.

The ZoneEarthTube object in EnergyPlus enables the integration of the EAHE system into the simulation. The calculation of the EAHE air volumetric flow rate (ET_{FR}) used by the software is defined as follows [42]:

$$ET_{FR} = \left(E_{design}\right)\left(F_{Schedule}\right)\left[A + B|T_{zone} - T_{odb}| + C(WindSpeed) + D\left(WindSpeed^2\right)\right] \quad (4)$$

where E_{design} is the volumetric airflow rate inside the duct; $F_{Schedule}$ is the schedule that modulates the airflow rate in the duct; A is the dimensionless ground thermal constant; B is the temperature difference between the indoor and outdoor dry-bulb air temperatures; $|T_{zone} - T_{odb}|$ is the absolute temperature difference between indoor and outdoor dry-bulb air temperatures, below which the EAHE system is deactivated; C is the air velocity acting outside the building; *WindSpeed* is the air velocity within the duct; and D is the square of the wind speed acting outside the building.

In addition to the climate file for the study region, it is also necessary to input the average ground surface temperature, the ground surface temperature amplitude, and the ground surface temperature phase constant, which is the time elapsed from the beginning of the year until the ground surface temperature reaches its annual minimum. These parameters must be calculated in advance using a separate standalone program (CalcSoilSurfTemp) and then entered into EnergyPlus.

CalcSoilSurfTemp is a program already included in EnergyPlus and requires only two input fields: a file with soil conditions and another containing the surface soil conditions based on climatic conditions. The program calculates the thermal diffusivity and thermal conductivity of the soil surrounding the duct, as well as the absorption coefficient and evaporation rate at the soil surface. These calculations are based on the information provided in the SoilCondition field. This determines the thermal diffusivity and conductivity of the surrounding soil, which are related to the amount of heat transferred from the soil to the air flowing through the EAHE [42].

In the present simulations, the soil model was based on heat transfer between the air flowing through the EAHE duct and the surrounding soil. Dynamic moisture transport in the soil was not explicitly solved. The influence of soil conditions, including the effect of moisture content, was indirectly represented through the soil thermophysical properties adopted for each representative location and through the soil surface parameters calculated with CalcSoilSurfTemp. Therefore, the soil surrounding the EAHE was treated as an equivalent thermal medium characterized by its thermal conductivity, thermal diffusivity, density, specific heat capacity, average soil surface temperature, temperature amplitude, and phase constant. The duct was assumed to be straight, buried at the prescribed depth, and operated with a constant airflow velocity, while the interaction between the EAHE and the building thermal zones was modeled using the ZoneEarthTube object in EnergyPlus. These assumptions are consistent with the objective of evaluating the thermoenergetic impact of EAHE integration into SH under different Brazilian bioclimatic conditions.

To represent the six BZs, weather files from representative cities of each zone are used. The selected cities are Curitiba—PR (BZ1M), Viamão—RS (BZ2R), Brasília—DF (BZ3B), Goiânia—GO (BZ4B), Cuiabá—MT (BZ5B), and Recife—PE (BZ5A).

These representative cities are chosen based on several key criteria: (I) obtaining SPT data; (II) weather files from the standard database described in ABNT TR 15575 [40]; (III) use of TRY-type climate files, since the Test Reference Year (TRY) is considered ideal for bioclimatic assessments [44], while Climatological Normals from INMET may be used when TRY data are unavailable; (IV) availability of extensive climatic data; and (V) status as state capitals.

The weather files used provide monthly values of average soil temperature for all months of the year, as well as the following representative hourly data for the 8760 h of the typical meteorological year: (I) dry-bulb temperature; (II) dew point temperature; (III) relative humidity; (IV) atmospheric pressure; (V) longwave horizontal radiation intensity; (VI) global horizontal radiation; (VII) direct normal radiation; (VIII) diffuse horizontal radiation; (IX) wind direction, measured clockwise from true north; and (X) wind speed.

The EnergyPlus software presents some limitations and challenges: (I) the EAHE system allows only a single duct per thermal zone and restricts the duct to a straight configuration; (II) there are limited options for soil types in the CalcSoilSurfTemp tool; and (III) the software does not support simulations involving two different types of natural ventilation, such as combining *ZoneEarthTube* (implementation of the EAHE in the program) with the *Airflow Network* (calculated natural ventilation).

https://doi.org/10.3390/buildings16112285

2.7. Evaluation of the Thermoenergetic Performance of the SH with the Installation of the EAHE

After evaluating the thermoenergetic performance of the SH in accordance with NBR 15575 [40], the actual SH model is used in both the best and worst configurations in terms of solar orientation, and the EAHE system is coupled to investigate its performance. The parameters *PHFT* and *CgTT* are analyzed.

This evaluation considers the building occupancy according to NBR 15575 [40], as well as a scenario with 100% occupancy.

Finally, after all these analyses, a comparative assessment of the results is carried out to evaluate the effects of solar orientation, bioclimatic conditions, and EAHE installation on the thermoenergetic performance of the SH.

3. Results

This section presents the results of the computational model verification and validation procedures, as well as the investigation of the thermoenergetic performance of the SH across the different BZs.

3.1. Results of the Verification and Validation of the Computational Model

The verification and validation of the computational model developed in EnergyPlus consist of analyzing the thermal behavior through the daily average temperature values of the EAHE ducts (A, B, and C) and the building zones (A and B) of the Casa Ventura building (Figure 2).

To do so, the computational model was verified against the numerical results presented in [36] and validated against the experimental data presented in [34,35]. These comparisons analyze the temperature variations at the duct outlets and inside the building zones of the computational model throughout the year 2007. To facilitate the comparison between the results, the actual data are converted into a trend line for both the ducts and the building zones, where it is observed that the curve type that best fits the existing data is sinusoidal.

It is worth mentioning that the verification and validation indicators were calculated from annual temperature curves obtained using daily average values. The adoption of daily averages reduces the influence of short-term fluctuations and allows a more consistent comparison among experimental measurements, previous numerical results, and the present EnergyPlus simulations. The relative difference was used in the verification step, comparing the present EnergyPlus results with previous numerical results obtained with ANSYS FLUENT 6.3, whereas the relative error was used in the validation step, comparing the present results with the experimental data reported for Casa Ventura. For the EAHE system, the outlet air temperatures of ducts A, B, and C were evaluated, while for the building thermal response, the indoor air temperatures of zones A and B were analyzed. These indicators were calculated based on the deviations between the annual temperature trends of the compared datasets. Therefore, the verification procedure assessed the numerical consistency of the EAHE model, while the validation procedure assessed both the duct outlet air temperature and the indoor thermal response of the coupled EAHE-building system.

3.1.1. Ducts

The computational model of the EAHE is verified through comparison with the numerical study [36], which uses the FLUENT software, resulting in a relative difference of 0.83% for duct A, 0.72% for duct B, and 0.09% for duct C.

In turn, the validation of the computational model of the EAHE is performed by comparing it with the experimental results reported in [34], achieving a relative error of 0.87% for duct A, 0.62% for duct B, and 3.17% for duct C, as shown in Figures 5–7.

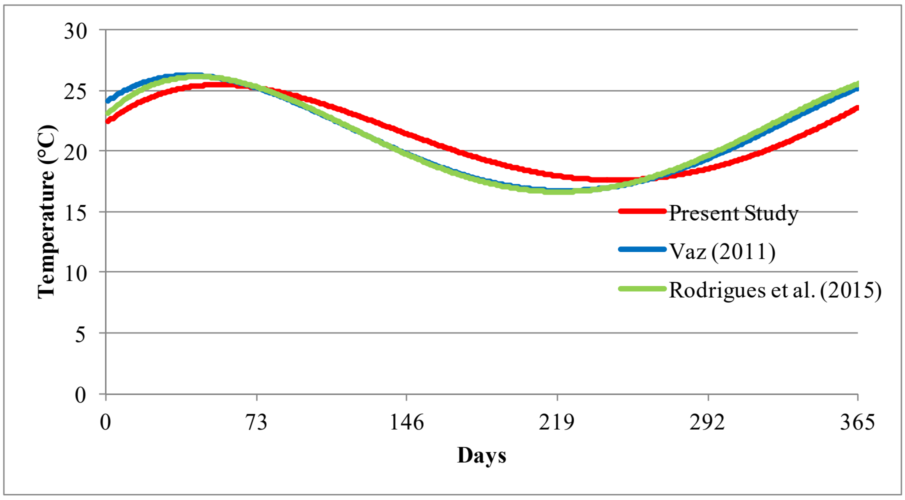

Figure 5. Graph of the transient temperature behavior at the outlet of duct A, compared with Vaz et al. [35] and Rodrigues et al. [36].

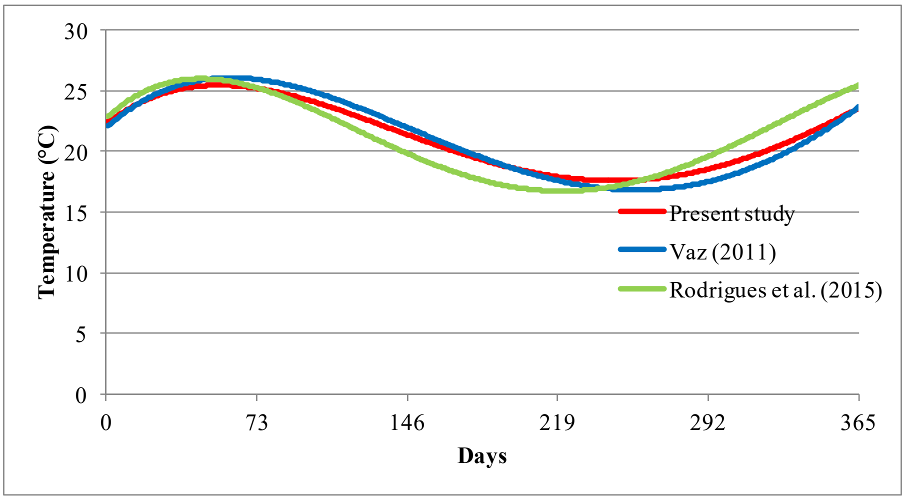

Figure 6. Graph of the transient temperature behavior at the outlet of duct B, compared with Vaz et al. [35] and Rodrigues et al. [36].

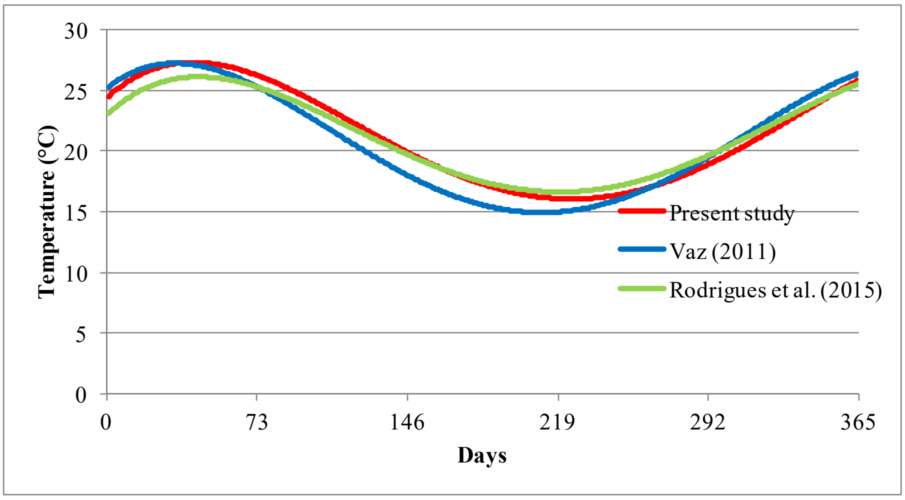

Figure 7. Graph of the transient temperature behavior at the outlet of duct C, compared with Vaz et al. [35] and Rodrigues et al. [36].

https://doi.org/10.3390/buildings16112285

In light of the results obtained in this study, it is possible to infer that the computational model for the numerical simulation of the EAHE in EnergyPlus has been properly verified and validated.

3.1.2. Zones

The building zones are only validated, since no numerical simulations have yet been conducted for Casa Ventura. Therefore, when comparing the numerical results obtained in this work with the experimental results reported in [34], differences of 3.40% in zone A and 4.24% in zone B were found, as shown in Figure 8.

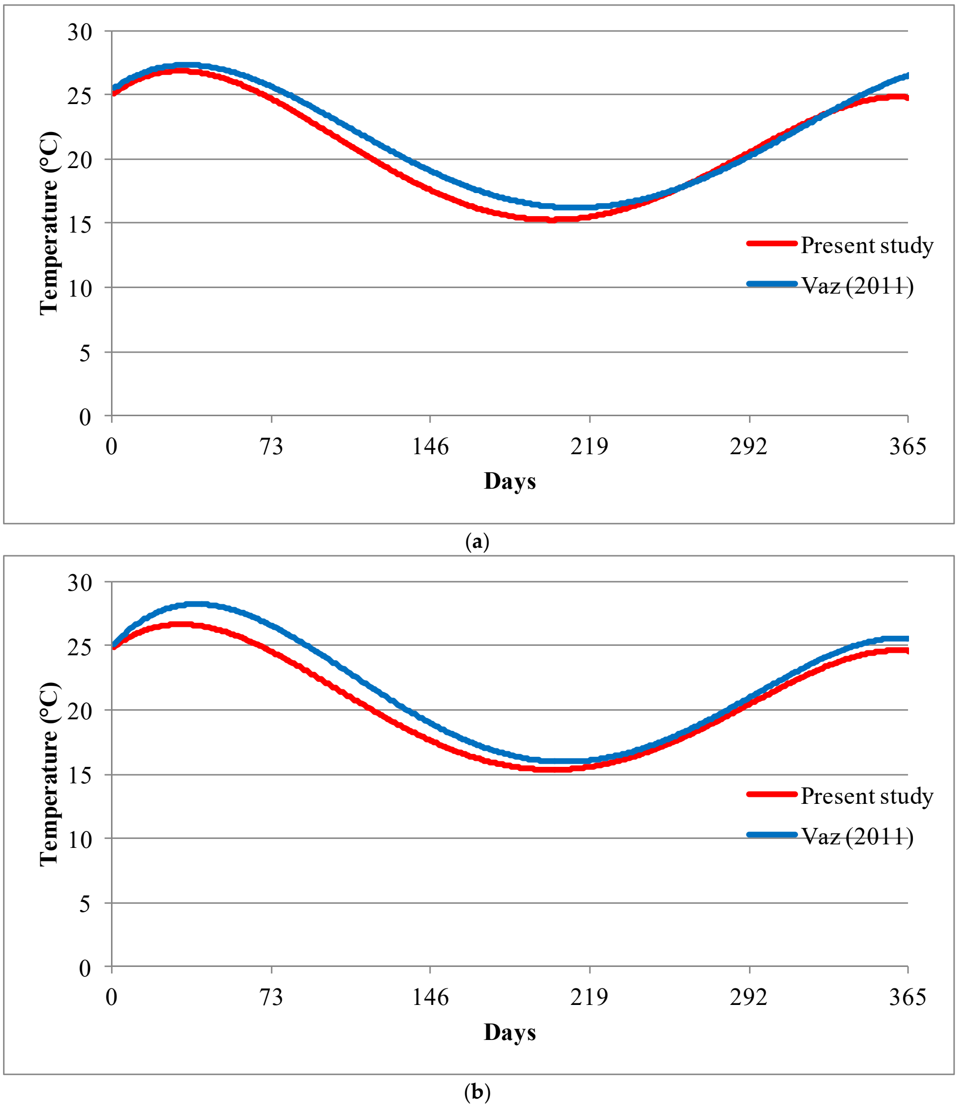

Figure 8. Graph of the temperature behavior inside the building zones: (**a**) zone A and (**b**) zone B, compared with Vaz [34].

In view of this, the computational model developed in EnergyPlus for the coupled simulation of the EAHE in built environments was properly validated, achieving relative errors below 5%.

3.2. Evaluation of the Thermoenergetic Performance of the SH for Each BZ

Using the computational simulation procedure outlined in NBR 15575 [40], two models are evaluated: the actual model, which preserves the geometric characteristics of the SH, the thermal properties, and the composition of the transparent elements, walls, and roof; and the reference model, which represents the same building but with standardized reference characteristics, as shown in Table 3.

From Table 3, it can be observed that the actual model, when compared to the reference model, has walls and roofs with lower thermal transmittance, meaning that it offers greater thermal insulation. Additionally, the actual model also presents lower absorptance values, meaning it absorbs less heat into the building.

Summarized results for all analyzed BZ will be presented, while detailed results will be provided only for BZ2R, as it corresponds to the same zone used in the computational verification and validation.

3.2.1. BZ2R

BZ2R is represented by the city of Viamão, RS. Several data sources, including experimental data, are available for this location, facilitating the comparative analysis. This zone recommends the following bioclimatic design strategies: in summer, cross ventilation; and in winter, solar heating of the building and the use of heavy internal partitions (thermal inertia). Additionally, medium-sized ventilation openings (15% < A < 25%) are recommended, as well as window shading that allows solar radiation to enter only during winter. Furthermore, walls with $U \leq 3.6$ (light reflective walls) and roof with $U \leq 2.0$ (light insulated roofs), according to NBR 15220 [33]. In turn, the adopted soil data are presented in Table 2.

The weather file for Viamão—RS (Figure 9) shows an annual average outdoor Dry-Bulb Temperature (*DBTm*) of 19.5 °C. Therefore, according to NBR 15575 [40], this value falls within the acceptable range of 18.0 °C to 26.0 °C for the operative temperature of the Housing Unit (UH), meaning it can potentially provide thermal comfort for the occupants. Temperatures above this range may result in heat discomfort, while temperatures below it may cause cold discomfort.

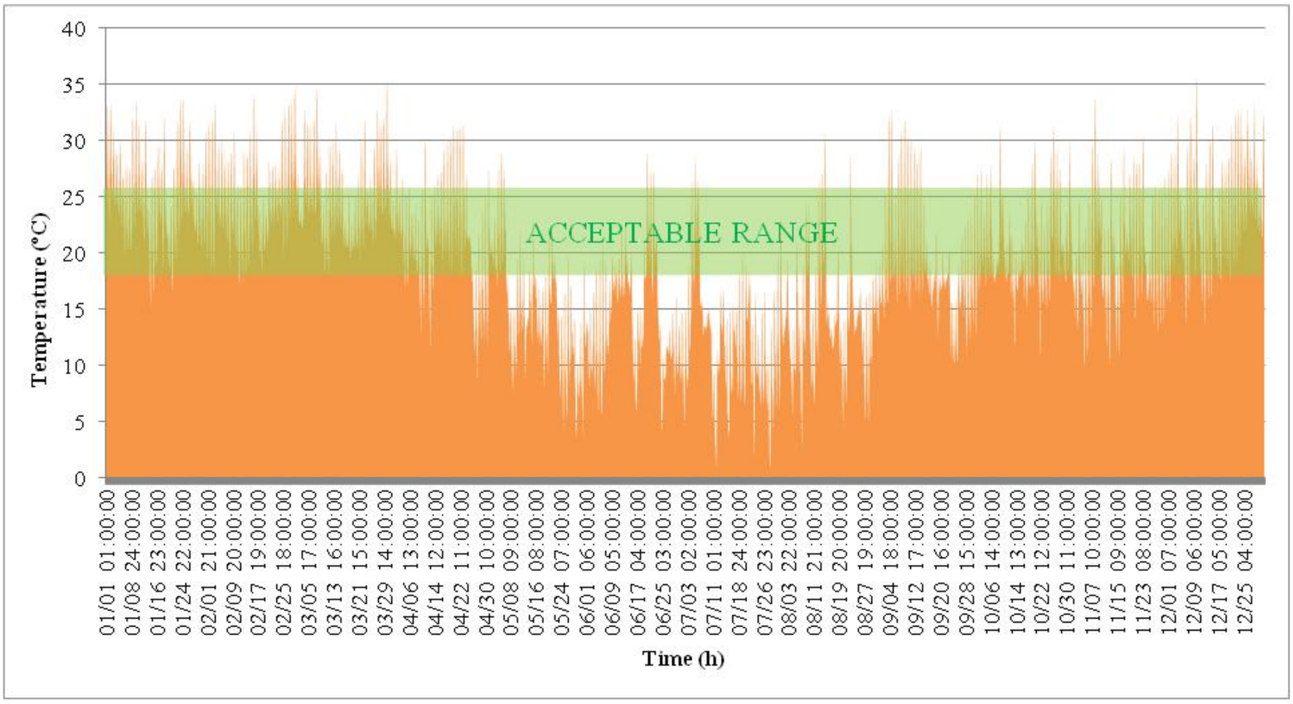

Figure 9. Representative graph of the outdoor dry-bulb temperature from the weather file of Viamão—RS, over one year, on an hourly basis.

From a thermal performance perspective, when comparing the simulation results of the actual model with the reference model in BZ2R, it is observed that the real SH model shows greater cold discomfort than heat discomfort (see Figure 10 and Tables 4 and 5). This is due to its higher insulation and lower absorptance, which prevent heat from entering the building zones. In contrast, the reference model, which is less insulated and uses materials with higher absorptance, exhibits greater heat discomfort.

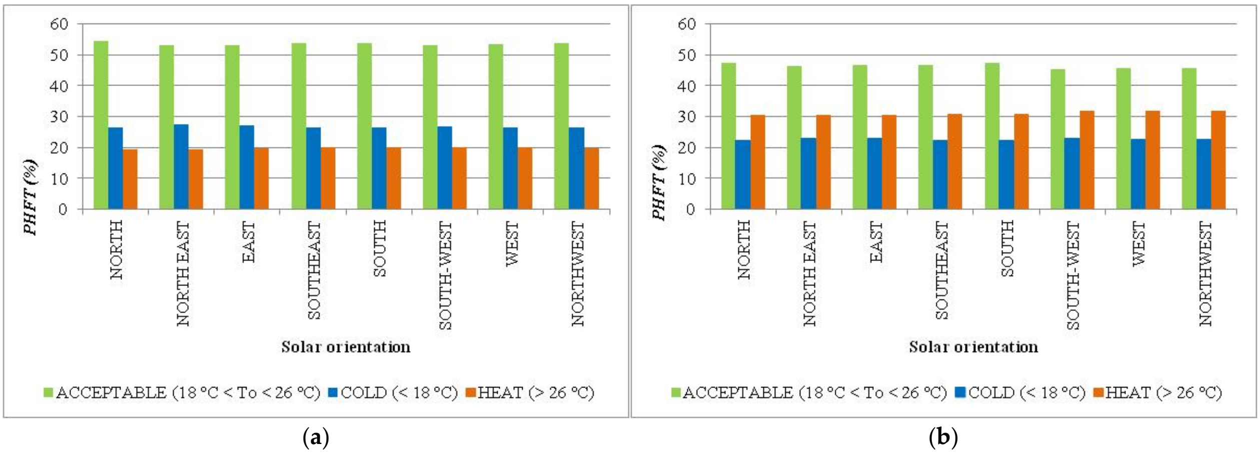

Figure 10. Graph of *PHFT* variation in BZ2R for the: (**a**) real model and (**b**) reference model.

Table 4. Results of all analyzed parameters related to the thermal performance of the real model (BZ2R).

Real Model: Climate Archive VIAMÃO—RS								
***PHFTUH* (%)**	**N**	**NE**	**E**	**SE**	**S**	**SW**	**W**	**NW**
Acceptable (18 °C < *To* < 26 °C)	54.2	53.1	53.1	53.7	53.8	53.0	53.5	53.8
Cold (<18 °C)	26.5	27.4	27.1	26.4	26.3	26.9	26.5	26.4
Heat (>26 °C)	19.2	19.5	19.8	19.9	19.9	20.1	20.0	19.8
To max (°C)	32.7	33.1	33.2	33.2	32.9	32.9	32.9	32.8
To min (°C)	11.4	11.1	11.0	11.0	11.1	11.2	11.4	11.4

Table 5. Results of all analyzed parameters related to the thermal performance of the reference model (BZ2R).

Reference Model: Climate Archive VIAMÃO—RS								
***PHFTUH* (%)**	**N**	**NE**	**E**	**SE**	**S**	**SW**	**W**	**NW**
Acceptable (18 °C < *To* < 26 °C)	47.3	46.3	46.8	46.8	47.2	45.4	45.5	45.6
Cold (<18 °C)	22.3	23.1	22.8	22.3	22.1	22.9	22.6	22.5
Heat (>26 °C)	30.4	30.6	30.4	30.8	30.7	31.7	31.9	31.8
To max (°C)	34.7	35.6	35.9	35.4	34.6	34.8	34.4	34.8
To min (°C)	11.8	11.8	12.0	12.0	12.2	12.3	12.4	12.0

However, the real model shows better thermal performance compared to the reference model, reaching up to an 8.2% difference within the acceptable range. In other words, materials with lower transmittance and absorptance values enable better thermal performance for this SH model in BZ2R.

In addition to these results, it is also observed that the best solar orientation is north, with a difference of 1.2% compared to the worst orientation, which is southwest. Finally, in the thermal performance assessment of the building envelope based on the *PHFT* criterion for the SH in BZ2R, all solar orientations meet the minimum performance level. However, according to the criteria for maximum and minimum annual operative temperatures, the south and southwest orientations do not meet the minimum performance level.

From an energy performance perspective, when comparing the simulation results of the real model with the reference model in BZ2R, it is evident that both models exhibit higher cooling loads than heating loads (Figure 11). However, the actual model shows a significantly lower cooling load, with a difference of 1454.80 kWh/year compared to the reference model for the southeast orientation, as shown in Table 6.

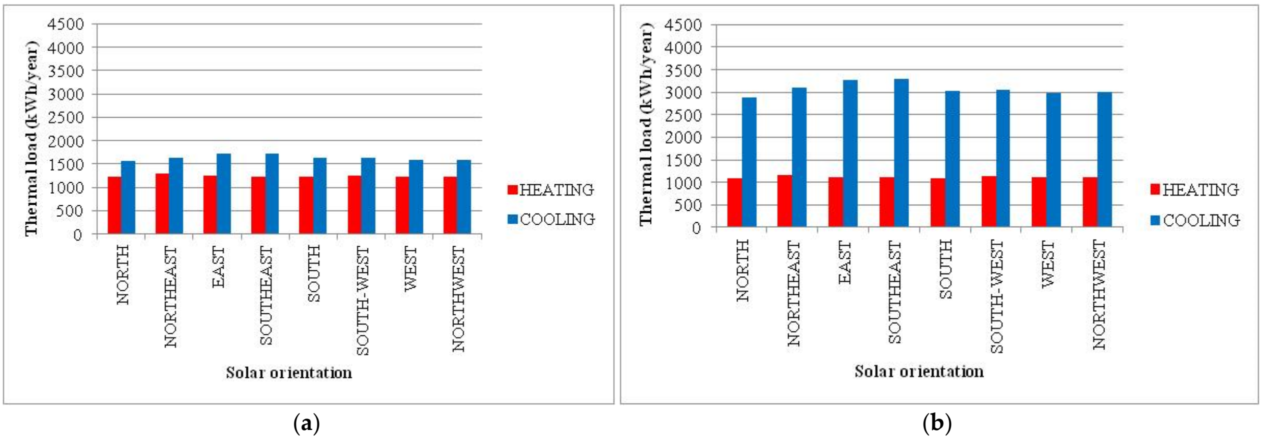

Figure 11. Graph of heating and cooling loads in BZ2R for the: (**a**) real model and (**b**) reference model.

Table 6. Total thermal load in the real and reference models in BZ2R, in kWh/year.

	N	NE	E	SE	S	SW	W	NW
Real	2783.44	2923.50	2988.56	2949.57	2857.30	2875.45	2819.42	2801.03
Reference	3990.41	4250.46	4392.96	4404.36	4132.26	4193.70	4099.71	4110.71

Therefore, it can be inferred that the real model demonstrates better energy performance than the reference model. Additionally, it is observed that the best solar orientation is north, with a difference of 205.13 kWh/year when compared to the worst orientation, which is east.

Based on the presented thermoenergetic performance results (see Figure 11 and Table 6), it is noted that in the south and southwest orientations, this SH does not meet the minimum performance level according to NBR 15575 [40], despite this being a requirement in Brazilian government programs for this type of construction.

Nevertheless, this SH model complies with the recommended ideal ventilation opening areas and meets the recommended thermal transmittance values for walls and roofs. However, in accordance with NBR 15220 [33], to improve the thermoenergetic performance of this SH model in BZ2R, the bioclimatic strategies indicated in Table 7 are recommended.

In addition to the bioclimatic strategy recommendations according to the standard, proper siting of this SH model is also suggested, as solar orientation plays a fundamental role in the building's thermal performance, potentially causing it to fail to meet the minimum performance level.

For the evaluation of the thermal performance of the SH with the EAHE coupled, it was necessary to calibrate the air changes per hour, due to a limitation in the EnergyPlus software when combining the EAHE (ZoneEarthTube) with the calculated natural ventilation (Airflow Network). The software does not support both types of natural ventilation simultaneously, thus preventing the numerical simulation. However, it accepts simplified ventilation, which considers windows without operation and a constant infiltration rate (Zone Ventilation: Design Flow Rate). Therefore, calibration of the air change per hour (ACH) was required to achieve results closer to those of the calculated natural ventilation using the simplified method. These results are shown in Table 8, indicating that the best result for BZ2R is 10 ACH.

Table 7. Bioclimatic Strategies for BZ2R.

In Summer:	**In Winter:**	
Cross ventilation	Passive solar heating	Thermal inertia for heating (heavy internal seals)
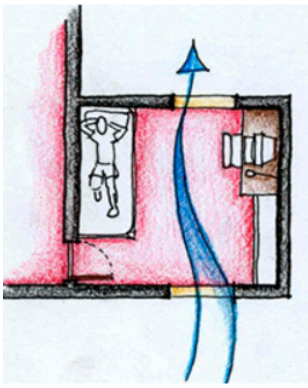	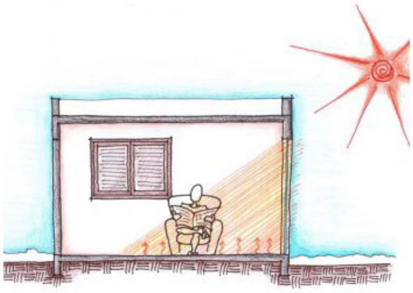	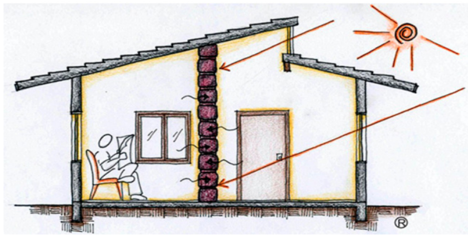

Table 8. Calibration of BZ2R.

	Calibration	
	Number of ACH	***PHFT*** **(%)**
Calculated Ventilation		54.2
Simplified Ventilation	20	50.8
	16	50.9
	14	50.9
	12	51.0
	10	51.0
	8	50.9

It is important to highlight that from a building physics perspective, the adoption of 10 ACH represents an equivalent ventilation rate capable of reproducing, with the simplified ventilation model, the thermal behavior obtained with calculated natural ventilation. This value provides sufficient air renewal to influence the operative temperature of the occupied zones while maintaining the pre-conditioning effect promoted by the EAHE. Lower ACH values reduce the amount of conditioned air supplied to the indoor environment, limiting the impact of the EAHE on the thermal zone. Conversely, excessively high ACH values may reduce the residence time of air inside the buried ducts and increase the influence of outdoor air conditions, thereby decreasing the effectiveness of the heat exchange with the soil. Therefore, 10 ACH was adopted as the calibrated value that best represents the compromise between air renewal, duct heat exchange, and indoor thermal response for BZ2R.

Based on the previous analyses (see Figures 10a and 11a and Tables 4 and 6), the best and worst thermal and energy performance results in the real model, regarding solar orientation, were considered, and the EAHE was installed in the SH to investigate its behavior. The parameters *PHFT* and *CgTT* were evaluated.

Analyzing the annual results, it is observed that for *PHFT*, both in the best solar orientation (north) and the worst (southwest), the use of the EAHE enhances the thermal performance of the SH by 4.5% (as shown in Table 9), demonstrating the system's efficiency. This difference corresponds to seventeen additional days per year with thermal comfort for the occupants, i.e., within the acceptable range according to the current standard.

Table 9. *PHFT* variation in the best and worst solar orientations, with and without the use of the EAHE, in BZ2R.

	PHFT (%)			
	Best Orientation (N)		Worst Orientation (SW)	
	Without EAHE	With EAHE	Without EAHE	With EAHE
Acceptable (18 °C < *To* < 26 °C)	51.0	55.6	50.4	54.9
Cold (<18 °C)	30.9	29.2	30.9	29.1
Heat (>26 °C)	18.0	15.3	18.8	16.1
Difference	4.5		4.5	

Subsequently, still regarding *PHFT*, a monthly analysis of the building is conducted, with and without the EAHE, in the best orientation (north), considering 100% occupancy. It is observed that in all months the values are more acceptable with the EAHE than without the device. However, in January, May, June, November, and December, the EAHE performs significantly better than in the other months, achieving up to a 7.8% improvement in the percentage of occupied hours within the acceptable operative temperature range, as shown in Figure 12.

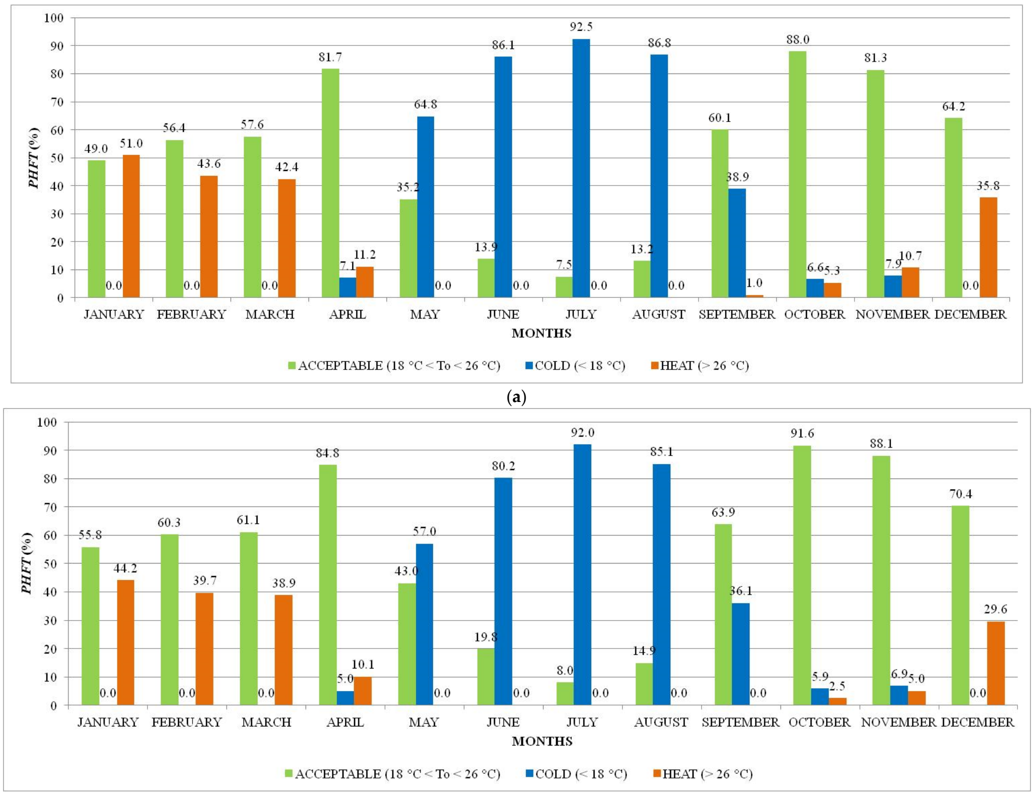

(**a**)

(**b**)

Figure 12. Comparison of *PHFT* variation in the best solar orientation, considering 100% occupancy in BZ2R: (**a**) without the EAHE and (**b**) with the EAHE.

In the month with the best performance, which is May (see Figure 12), a trend line is drawn to compare the outdoor temperature, the operative temperature inside the room, and the temperature at the duct outlet. It is observed that the temperature at the duct outlet remains constant, averaging 22.6 °C, and that the operative temperature inside the room approaches this temperature, which explains the best results, as shown in Figure 13.

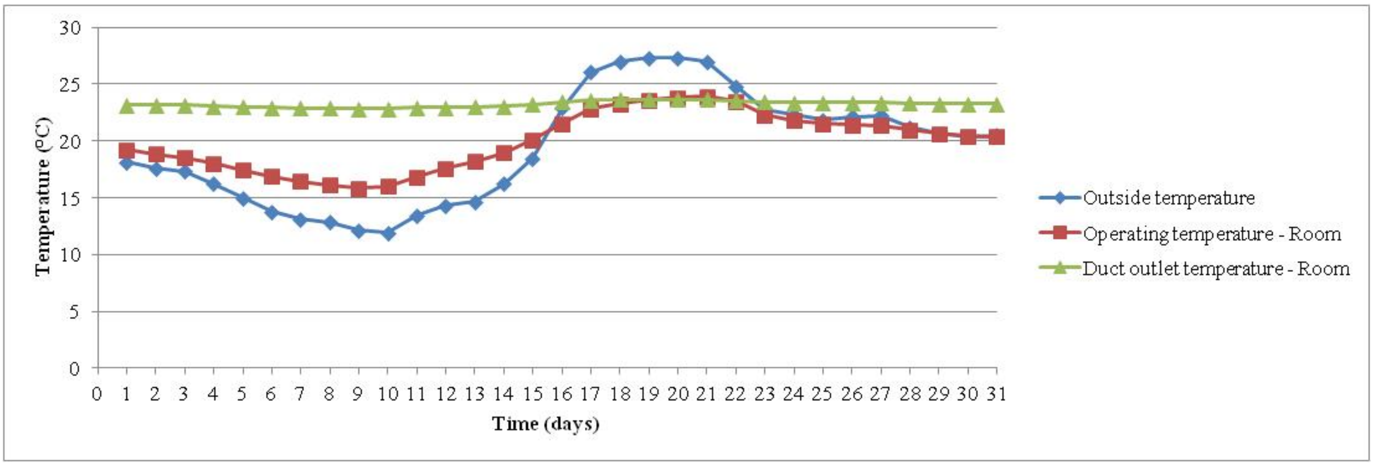

Figure 13. Representative graph for the month of May, in the best solar orientation scenario, considering 100% occupancy in BZ2R.

It should be noted that the temperature evolution presented in Figure 13 is discussed on a representative monthly basis rather than as an intraday profile for a specific 24 h period. Although the EnergyPlus simulations were performed using hourly climatic and thermal data, the performance assessment adopted in this study is based on annual and monthly indicators, especially *PHFT* and *CgTT*. Therefore, the temperature curves are used to support the interpretation of the monthly thermoenergetic behavior of the SH with and without the EAHE. In general, the EAHE tends to attenuate the influence of outdoor temperature fluctuations on the indoor environment, since the air supplied through the buried ducts exchanges heat with the soil before entering the building. As a result, the EAHE outlet temperature is less sensitive to short-term outdoor temperature variations, contributing to a smoother indoor operative temperature behavior and improved thermal comfort in the months in which the system presents favorable performance.

Regarding the *CgTT* criterion, analyzing the annual results shows that both solar orientations analyzed (north and east) increase the total thermal load with the use of the EAHE, as shown in Table 10.

Table 10. Variation of *CgTT* in the best and worst solar orientations, with and without the use of the EAHE, in BZ2R.

CgTT (kW/Year)				
	Best Orientation (N)		**Worst Orientation (SW)**	
	Without EAHE	**With EAHE**	**Without EAHE**	**With EAHE**
Heating	1121.89	1066.32	1167.14	1097.88
Cooling	1366.05	1806.08	1537.00	1985.65
Total	2487.94	2872.41	2704.14	3083.52
Difference	−384.47		−379.38	

Based on this evaluation regarding *CgTT*, a monthly analysis of the building is conducted with and without the EAHE, in the best solar orientation, and it is observed that in the months of May, June, and July the energy performance of the SH improves with the use of the EAHE, as shown in Table 11.

Table 11. Monthly *PHFT* and *CgTT* Results for BZ2R.

		JAN	FEB	MAR	APR	MAY	JUN	JUL	AUG	SEP	OCT	NOV	DEC
PHFT (%)													
Without EAHE	Acceptable (18 °C < To < 26 °C)	49.0	56.4	57.6	81.7	35.2	13.9	7.5	13.2	60.1	88.0	81.3	64.2
	Cold (<18 °C)	0.0	0.0	0.0	7.1	64.8	86.1	92.5	86.8	38.9	6.6	7.9	0.0
	Heat (>26 °C)	51.0	43.6	42.4	11.2	0.0	0.0	0.0	0.0	1.0	5.3	10.7	35.8
With EAHE	Acceptable (18 °C < To < 26 °C)	55.8	60.3	61.1	84.8	43.0	19.8	8.0	14.9	63.9	91.6	88.1	70.4
	Cold (<18 °C)	0.0	0.0	0.0	5.0	57.0	80.2	92.0	85.1	36.1	5.9	6.9	0.0
	Heat (>26 °C)	44.2	39.7	38.9	10.1	0.0	0.0	0.0	0.0	0.0	2.5	5.0	29.6
	Difference	6.8	3.9	3.5	3.1	7.8	5.9	0.5	1.7	3.8	3.6	6.8	6.2
	Days	2.1	1.1	1.1	0.9	2.4	1.8	0.2	0.5	1.1	1.1	2.0	1.9
CgTT (kWh)													
Without EAHE	Heating	0.00	0.00	0.00	0.39	144.30	289.92	362.47	294.31	30.39	0.00	0.10	0.00
	Cooling	363.27	285.96	276.79	51.58	0.00	0.00	0.00	0.00	0.00	26.12	91.47	270.85
	Total	363.27	285.96	276.79	51.98	144.30	289.92	362.47	294.31	30.39	26.12	91.57	270.85
With EAHE	Heating	0.00	0.00	0.00	0.23	111.19	243.27	353.27	317.86	40.22	0.00	0.29	0.00
	Cooling	462.47	405.39	423.23	76.84	0.00	0.00	0.00	0.00	0.00	27.30	96.10	314.75
	Total	462.47	405.39	423.23	77.08	111.19	243.27	353.27	317.86	40.22	27.30	96.39	314.75
	Difference	−99.20	−119.43	−146.44	−25.10	33.11	46.65	9.21	−23.55	−9.83	−1.17	−4.81	−43.90

Finally, evaluating the feasibility of the EAHE system regarding the thermoenergetic performance of the SH, it was inferred that the system is efficient from May to November, but not in the remaining months. This is evidenced by the additional days each month with occupants' thermal comfort, as shown in Table 11.

3.2.2. Summary of the Thermoenergetic Performance Evaluation of the SH for Each BZ

In summary, it is observed that the improvement in thermoenergetic performance is more effective in terms of thermal comfort than in the thermal load of the SH. Through the monthly analysis of the EAHE performance, it is possible to determine the system's feasibility. Therefore, the EAHE system coupled to the SH building improves thermoenergetic performance in BZ1M for six months (from November to April); in BZ2R for seven months (from May to November); in BZ3B for six months (from May to October); and in BZ4B for five months (from May to September). Conversely, in BZ5B and BZ5A, the system proves inefficient due to the few additional days per month with occupants' thermal comfort, as shown in Table 12.

From a physical point of view, the better performance of the EAHE in BZ1M, BZ2R, BZ3B, and BZ4B is mainly associated with the greater useful temperature difference between the outdoor air and the surrounding soil during relevant periods of the year. Under these conditions, the soil can act more effectively as a heat source during colder periods and as a heat sink during warmer periods, enhancing the convective heat transfer rate inside the buried ducts. This allows the air flowing through the ducts to approach a more favorable temperature before entering the building. In contrast, in warmer zones such as BZ5B and BZ5A, the persistently high outdoor temperatures and the consequent higher baseline soil temperatures reduce the effective temperature gradient between the air and the soil. This narrow thermal gradient limits the conductive heat dissipation into the ground and can reduce the capacity of the soil surrounding the ducts to absorb additional heat during extended operation. As a result, the outlet air temperature tends to provide a less significant improvement in indoor thermal conditions, which explains the lower thermoenergetic effectiveness observed in these zones.

Table 12. Synthesis of the Annual Results for Each BZ.

BZ	Representative Cities	*DBTm*	Results (Differences with and Without EAHE)					Compliance with Current NBRs		Feasibility of the EAHE System
			PHFT			CgTT				
			%	Days/Year	Favorable Months	kWh/ano	Favorable Months	15575-1 (2021)	15220-3 (2005)	
1M	CURITIBA—PR	16.3°	2.2	8.0	From November to May	−388.36	Jan/Mar/Dec	x	✓	✓ (6 months)
2R	VIAMÃO—RS	19.5°	4.5	16.4	All	−379.38	May/Jun/Jul	x	✓	✓ (7 months)
3B	BRASÍLIA—DF	21.3°	3.7	13.5	All	−207.23	Jun/Jul/Aug/Sep	x	x	✓ (6 months)
4B	GOIÂNIA—GO	23.2°	1.1	4.0	From April to September	−568.52	Jun/Jul/Aug	✓	x	✓ (6 months)
5B	CUIABÁ—MT	26.3°	1.4	5.1	From August to December	−1615.5	None	✓	x	x
5A	RECIFE—PE	25.7°	3.9	14.2	All	−1759.8	None	✓	x	x

From this synthesis, it is also evident that a single SH model (standard model) does not adapt to all Brazilian BZs nor meet the minimum requirements of current standards (NBR 15220 [33] and NBR 15575 [40]) regarding performance. Therefore, the importance of developing specific designs for each location is highlighted, respecting the climatic conditions and adhering to the constructive guidelines and bioclimatic strategies of each BZ. This approach promotes better thermoenergetic performance of SHs and avoids using standardized models nationwide, given the significant climatic diversity across the country.

In this context, it is observed that in the BZs with lower annual average outdoor dry-bulb temperatures ($DBTm \leq 23$ °C), the EAHE coupled to the building shows better results (BZ1M, BZ2R, BZ3B, and BZ4B), while in those with higher *DBTm* (≥24 °C), the results are poorer (BZ5B and BZ5A) in terms of thermoenergetic performance.

Analyzing the climates of Brazil, it is observed that the representative cities of BZ1M (Curitiba—PR), and BZ2R (Viamão—RS) are located in the subtropical climate zone, situated in the southern region of the country, below the Tropic of Capricorn. This climate is characterized by two well-defined seasons: hot summers and harsh winters, during which frost or even snow may occur. The annual average temperatures are generally below 18 °C, with thermal amplitudes ranging between 9 °C and 13 °C.

In accordance with the results presented, there is a noticeable trend of adequate thermoenergetic performance of the EAHE system under this type of climate. This finding aligns with [45], which reports that EAHE systems can improve indoor thermal comfort and reduce heating and cooling energy demand when climatic conditions are favorable to EAHE.

Another climate that showed favorable results regarding the thermoenergetic performance of the EAHE system is the high-altitude tropical climate, represented by BZ3B (Brasília—DF). This climate is found in regions located above 800 m of altitude on the Atlantic Plateau in the Southeast region of Brazil, encompassing all states in that area. It is strongly influenced by the Atlantic tropical air mass, which causes heavy rainfall during the summer. Average temperatures range between 18 °C and 22 °C, with thermal variations between 7 °C and 9 °C.

The tropical climate with a lower mean dry-bulb temperature ($DBTm \leq 23$ °C), represented by BZ4B (Goiânia—GO), shows results that indicate suitable thermoenergetic performance of the EAHE system. However, in the same climate type with a higher *TDBm* (≥24 °C), represented by BZ5B (Cuiabá—MT), satisfactory results were not achieved for this study. The same applies to the Atlantic tropical climate, represented by BZ5A (Recife—PE).

The other climate types were not evaluated in the present study. The Brazilian climate types and the representative cities of each BZ are illustrated in Figure 14 [46].

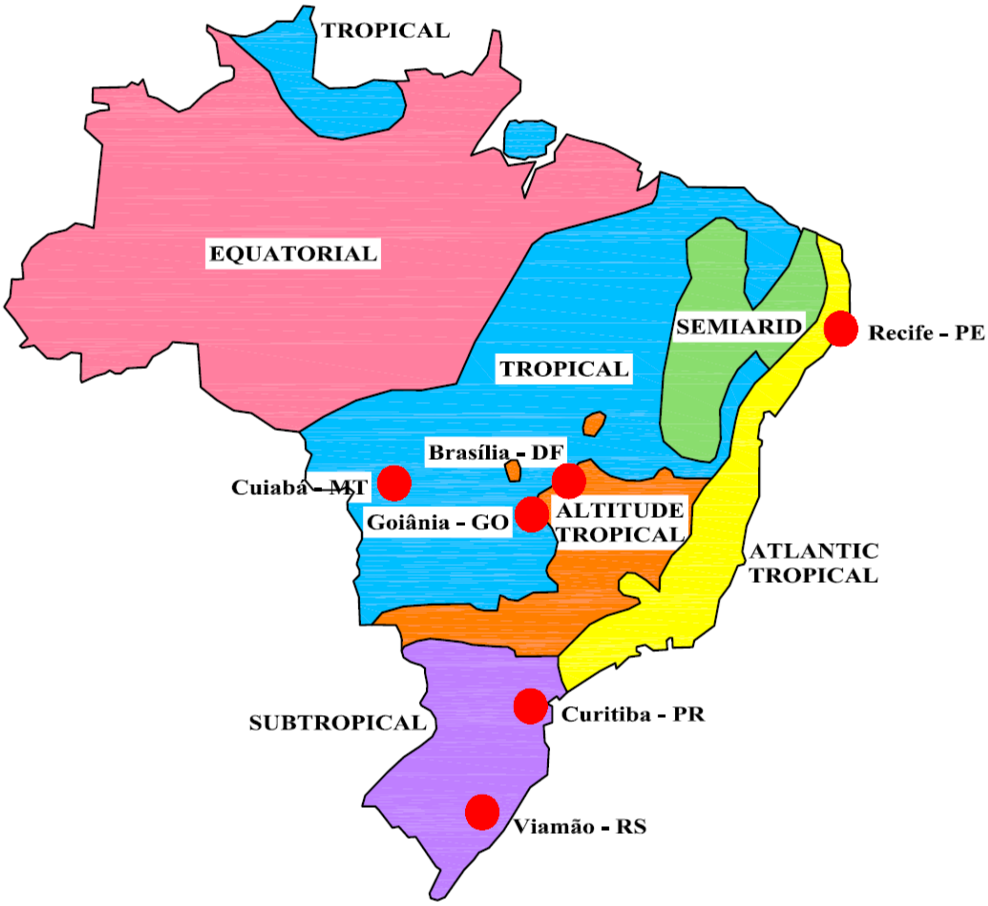

Figure 14. Map of Brazilian climates with the indication of the representative cities of each BZ.

4. Conclusions

This study evaluated the thermoenergetic performance of an EAHE system coupled to a SH building across different Brazilian BZs. The main conclusions are summarized as follows:

(I) The EnergyPlus computational model was successfully verified and validated using, respectively, numerical and experimental data available for the reference case, providing a novel contribution regarding EAHE systems integrated into SH buildings.
(II) The EAHE integration improved the thermoenergetic performance of the SH, showing a more pronounced impact on thermal comfort conditions than on thermal load reduction.
(III) Monthly analyses demonstrated that the EAHE was more effective in BZ1M, BZ2R, BZ3B, and BZ4B, but proved ineffective in BZ5B and BZ5A due to limited comfort gains and higher operating costs from fan energy consumption.
(IV) Considering only thermal performance, the EAHE yielded favorable annual results in all BZs. The highest *PHFT* improvement occurred in January for BZ1M, reaching 14.3%, equivalent to over four additional days per month within comfort limits.
(V) Regarding energy performance, the lowest monthly thermal load was achieved in June for BZ2R, reaching 46.65 kWh/month, reinforcing the system's energy-saving potential under specific operating conditions.

(VI) Building solar orientation significantly influenced performance, achieving thermal improvements of up to 3.3% and annual thermal load differences of up to 488.4 kWh/year without additional construction costs.
(VII) The standard SH design did not adequately adapt to all Brazilian BZs, failing to meet minimum national performance requirements and reinforcing the need for climate-responsive designs.
(VIII) The best EAHE performance occurred in subtropical, high-altitude tropical, and tropical climates with lower mean dry-bulb temperatures ($DBTm \leq 23$ °C), indicating higher effectiveness in cooler climates.
(IX) The proposed configuration can potentially be replicated in international regions outside Brazil sharing similar climatic characteristics.

Future research should focus on advanced EAHE configurations, integration with envelope insulation, occupant-related variables, and detailed soil characterization, including thermal conductivity, density, specific heat capacity, and moisture effects, to refine performance assessments. Future studies may also include a detailed intraday analysis of selected typical days. Such an analysis would allow a more specific evaluation of the hourly evolution of outdoor temperature, indoor operative temperature, and EAHE outlet temperature, providing further insight into daily peak attenuation and short-term thermal comfort improvement.

Author Contributions: Conceptualization, P.W.M., R.d.S.B. and L.A.I.; Methodology, P.W.M., M.W.M., R.d.S.B. and L.A.I.; Software, P.W.M. and R.d.S.B.; Validation, P.W.M., M.W.M. and L.A.I.; Formal analysis, P.W.M., L.A.O.R., E.D.d.S., R.d.S.B. and L.A.I.; Investigation, P.W.M. and L.A.I.; Resources, L.A.O.R., E.D.d.S., R.d.S.B. and L.A.I.; Data curation, P.W.M.; Writing—original draft, P.W.M.; Writing—review & editing, P.W.M., L.A.O.R., E.D.d.S., R.d.S.B. and L.A.I.; Visualization, L.A.O.R., E.D.d.S., R.d.S.B. and L.A.I.; Supervision, R.d.S.B. and L.A.I.; Project administration, L.A.I.; Funding acquisition, L.A.O.R., E.D.d.S., R.d.S.B. and L.A.I. All authors have read and agreed to the published version of the manuscript.

Funding: This research was funded by National Council for Scientific and Technological Development (CNPq), Brazil (Processes: 307791/2019-0, 308396/2021-9, and 309648/2021-1) and Research Support Foundation of the State of Rio Grande do Sul (FAPERGS), Brazil (Process: 21/2551-0002231-0).

Data Availability Statement: The original contributions presented in this study are included in the article. Further inquiries can be directed to the corresponding author.

Acknowledgments: L. A. O. Rocha, E. D. dos Santos, and L. A. Isoldi acknowledge CNPq for the research productivity fellowships (Processes: 307791/2019-0, 308396/2021-9, and 309648/2021-1, respectively). The authors also acknowledge the financial support provided by FAPERGS 07/2021—Researcher Gaúcho Program (PqG) (Process: 21/2551-0002231-0).

Conflicts of Interest: The authors declare no conflict of interest.

Nomenclature

The following table summarizes the main symbols, indicators, parameters, and acronyms used in the manuscript.

Symbol/Acronym	Description	Unit
A	Dimensionless ground thermal constant used in the ZoneEarthTube model	—
ACH	Air changes per hour	h^{-1}
A_i	Area of indoor surface i	m^2
APP	Prolonged Occupancy Area	—
B	Coefficient associated with the indoor-outdoor dry-bulb temperature difference in the ZoneEarthTube model	—
BZ	Bioclimatic Zone	—

Symbol/Acronym	Description	Unit
BZ1M, BZ2R, BZ3B, BZ4B, BZ5B, BZ5A	Brazilian bioclimatic zones considered in the study	—
C	Coefficient associated with wind-speed effects in the ZoneEarthTube model	—
$CgTAAPP$	Annual sum of hourly heating thermal load values in the APP	kWh/year
$CgTRAPP$	Annual sum of hourly cooling thermal load values in the APP	kWh/year
$CgTTUH$	Annual total thermal load of the housing unit	kWh/year
c_p	Specific heat capacity	J/kgK
C_z	Thermal zone heat capacity	J/K
D	Coefficient associated with the square of wind-speed effects in the ZoneEarthTube model	—
d	EAHE duct diameter	m
DBT	Dry-bulb temperature	°C
DBT_m	Mean dry-bulb temperature	°C
dT_z/dt	Time derivative of the zone air temperature	K/s or °C/s
EAHE	Earth-Air Heat Exchanger	—
E	East	—
E_{design}	Design volumetric airflow rate in the ZoneEarthTube model	m^3/s
F_1	Duct opening coefficient	—
F_2	Duct expansion coefficient	—
$F_{Schedule}$	Schedule factor that modulates the airflow rate through the EAHE duct	—
h	EAHE duct burial depth	m
h_i	Indoor convective heat transfer coefficient	W/m^2K
k	Thermal conductivity	W/mK
L	EAHE duct length	m
N	North	—
NE	Northeast	—
NW	Northwest	—
$PHFTAPP$	Percentage of occupied hours within the operative temperature comfort range in the APP	%
Q''	Heat flux per unit area	W/m^2
Q	Heat supplied or removed by the air system	W
q''_{cond}	Conductive heat flux	W/m^2
q''_{conv}	Convective heat flux	$W\ m^{-2}$
Q_i	Sum of convective internal heat loads	W
q''_{LWR}	Longwave radiative heat flux exchanged with the outdoor environment and surroundings	W/m^2
q''_{LWX}	Longwave radiative heat flux exchanged between thermal zone surfaces	W/m^2
q''_{sol}	Solar radiation heat flux absorbed by the surface	W/m^2
q''_{SW}	Shortwave radiative heat flux exchanged between thermal zone surfaces	W/m^2
SH	Social Housing	—
S	South	—
SE	Southeast	—
SW	Southwest	—
SPT	Standard Penetration Test	—
T	Temperature	K or °C
T_{ext}	Outdoor or external air temperature	K or °C
T_{in}	Indoor dry-bulb air temperature	K or °C
T_{odb}	Outdoor dry-bulb air temperature	K or °C
$T_{omax,APP}$	Annual maximum operative temperature in the APP	°C
$T_{omin,APP}$	Annual minimum operative temperature in the APP	°C
T_{si}	Indoor surface temperature of surface i	K or °C
T_z	Thermal zone air temperature	K or °C
TZ	Thermal Zone	—
T_{zone}	Indoor thermal zone air temperature	K or °C
UH	Housing unit (Unidade Habitacional)	—
W	West	—

Symbol/Acronym	**Description**	**Unit**
WindSpeed	Wind speed considered in the ZoneEarthTube model	m/s
A	Thermal diffusivity	m^2/s
ρ	Density	Kg/m^3
ρ_z	Zone air density	Kg/m^3

References

1. British Petroleum bp. *Statistical Review of World Energy 2021*; British Petroleum bp: London, UK, 2021; Volume 70. Available online: https://www.bp.com/content/dam/bp/business-sites/en/global/corporate/pdfs/energy-economics/statistical-review/bp-stats-review-2021-full-report.pdf (accessed on 13 December 2022).
2. Astina, I.M.; Nugraha, M.Y. Numerical simulation of earth-air heat exchanger application for Indonesian simple house air conditioning system. *Case Stud. Therm. Eng.* **2021**, *28*, 101371. [CrossRef]
3. Zeitoun, W.; Lin, J.; Siroux, M. Energetic and Exergetic Analyses of an Experimental Earth-Air Heat Exchanger in the Northeast of France. *Energies* **2023**, *16*, 1542. [CrossRef]
4. Benincá, L.; Sánchez, E.C.; Passuello, A.; Leitzke, R.K.; Cunha, E.G.; Barroso, J.M.G. Multi-objective optimization of the solar orientation of two residential multifamily buildings in south Brazil. *Energy Build.* **2023**, *285*, 112838. [CrossRef]
5. IEA. *Data and Statistics*; International Energy Agency: Paris, France, 2015.
6. BEN. Brazil, EPE. *National Energy Balance 2022: Base Year 2021-Final Report*; EPE: Rio de Janeiro, Brazil, 2022. Available online: http://www.epe.gov.br (accessed on 22 May 2025).
7. Ürge-Vorsatz, D.; Cabeza, L.F.; Serrano, S.; Barreneche, C.; Petrichenko, K. Heating and Cooling Energy Trends and Drivers in Buildings. *Renew. Sustain. Energy Rev.* **2015**, *41*, 85–98. [CrossRef]
8. Belloufi, Y.; Zerouali, S.; Rouag, A.; Aissaoui, F.; Atmani, R.; Brima, A.; Moummi, N. Transient assessment of an earth air heat exchanger in warm climatic conditions. *Geothermics* **2022**, *104*, 102442. [CrossRef]
9. Kaushal, M. Performance analysis of clean energy using geothermal earth to air heat exchanger (GEAHE) in Lower Himalayan Region–Case study scenario. *Energy Build.* **2021**, *248*, 111166. [CrossRef]
10. Hacini, K.; Benatiallah, A.; Harrouz, A.; Belatrache, D. Efficiency Assessment of an Earth-Air Heat Exchanger System for Passive Cooling in Three Different Regions-the Algerian Case. *FME Trans.* **2021**, *49*, 1035–1046. [CrossRef]
11. Mihalakakou, G.; Souliotis, M.; Papadaki, M.; Halkos, G.; Paravantis, J.; Makridis, S.; Papaefthimiou, S. Applications of earth-to-air heat exchangers: A holistic review. *Renew. Sustain. Energy Rev.* **2022**, *155*, 111921. [CrossRef]
12. Agostino, D.; Esposito, F.; Greco, A.; Masselli, C.; Minichiello, F. The Energy Performances of a Ground-to-Air Heat Exchanger: A Comparison Among Köppen Climatic Areas. *Energies* **2020**, *13*, 2895. [CrossRef]
13. Ahmed, S.F.; Khan, M.M.K.; Amanullah, M.T.O.; Rasul, M.G.; Hassan, N.M.S. Thermal performance of building-integrated horizontal earth-air heat exchanger in a subtropical hot humid climate. *Geothermics* **2022**, *99*, 102313. [CrossRef]
14. EL-Said, E.M.S.; Sharaf, M.A.; Aljabr, A.; Marzouk, S.A. Enhancing the performance of an earth air heat exchanger with novel pipe configurations. *Int. J. Heat Fluid Flow* **2024**, *110*, 109630. [CrossRef]
15. Cuny, M.; Lapertot, A.; Lin, J.; Kadoch, B.; Metayer, O. Multi-criteria optimization of an earth-air heat exchanger for different French Climates. *Renew. Energy* **2020**, *157*, 342–352. [CrossRef]
16. Zajch, A.; Gough, W.A. Seasonal sensitivity to atmospheric and ground surface temperature changes of an open earth-air heat exchanger in Canadian climates. *Geothermics* **2021**, *89*, 101914. [CrossRef]
17. Lapertot, A.; Cuny, M.; Kadoch, B.; Métayer, O.L. Optimization of an earth-air heat exchanger combined with a heat recovery ventilation for residential building needs. *Energy Build.* **2021**, *235*, 110702. [CrossRef]
18. Cirillo, L.; Greco, A.; Masselli, C. Daily, monthly and seasonal energy performances and economic assessment on the coupling of an earth to air heat exchanger to an already existing HVAC system: A case study for Italian cities. *Appl. Therm. Eng.* **2024**, *236*, 121884. [CrossRef]
19. Soares, T.A.; Langner, M.; Sacht, H.; Figueiredo, A.; Vicente, R. Multi-objective optimisation of an earth-to-air heat exchanger for thermal regulation in Southern Brazilian bioclimatic zones. *Energy Build.* **2025**, *347*, 116243. [CrossRef]
20. Yue, Y.; Yan, Z.; Lei, F.; Zhang, D.; Ni, P.; Yan, Y. Towards Climate-Adaptive Design: Performance Variations, Underlying Patterns, and Differentiated Strategies of Earth-Air Heat Exchangers across Diverse Climates in China. *Renew. Energy* **2026**, *269*, 125852. [CrossRef]
21. Ben Babba, K.; Sellami, M.; Ali, S. Earth-Air Heat Exchanger Systems for Energy Efficiency Enhancement in Algerian Residential Buildings: A Multi-Climate Zone Analysis. *Int. J. Comput. Exp. Sci. Eng.* **2026**, *12*, 1188–1204. [CrossRef]
22. Rodrigues, M.K.; Coswig, F.S.; Camargo, K.R.; Isoldi, L.A.; Brum, R.S.; Ramalho, J.V.A.; Vaz, J.; Rocha, L.A.O.; Santos, E.D. Thermal performance simulations of Earth-Air Heat Exchangers for different soils of a coastal city using in-situ data. *Sustain. Energy Technol. Assess.* **2018**, *30*, 224–229. [CrossRef]

23. Khachine, H.E.; Ouahabi, M.H.; Taoukil, D. Improvement of earth-to-air heat exchanger performance by adding cost-efficient soil. *Energy Explor. Exploit.* **2024**, *42*, 589–602. [CrossRef]
24. Pakari, A.; Ghani, S. Numerical evaluation of the thermal performance of a near-surface earth-to-air heat exchanger with short-grass ground cover: A parametric study. *Int. J. Refrig.* **2021**, *125*, 25–33. [CrossRef]
25. Long, T.; Zhao, N.; Li, W.; Wei, S.; Li, Y.; Lu, J.; Qiao, Z. Numerical simulation of diurnal and annual performance of coupled solar chimney with earth-to-air heat exchanger system. *Appl. Therm. Eng.* **2022**, *214*, 118851. [CrossRef]
26. Lechner, N. *Heating, Cooling, Lighting: Sustainable Design Methods for Architects*, 4th ed.; Wiley: Hoboken, NJ, USA, 2015.
27. Hsu, C.Y.; Huang, P.C.; Liang, J.D.; Chiang, Y.C.; Chen, S.L. The in-situ experiment of earth-air heat exchanger for a cafeteria building in subtropical monsoon climate. *Renew. Energy* **2020**, *157*, 741–753. [CrossRef]
28. João Pinheiro Foundation. *Housing Deficit in Brazil 2022*; João Pinheiro Foundation: Belo Horizonte, Brazil, 2023. Available online: https://repositorio.fjp.mg.gov.br/items/4ea6db72-4b2e-4dcb-af59-95202212ce9a (accessed on 14 May 2026).
29. Governo Federal do Brazil. *Provides for the "Minha Casa, Minha Vida" Program (PMCMV) and the Land Tenure Regularization of Settlements Located in Urban Areas*; Federal Law No. 11,977 of 7 July 7 2009; Governo Federal do Brazil: Brasília, Brazil, 2009.
30. Governo Federal do Brazil. *Establishes the Casa Verde e Amarela Program*; Federal Law No. 14,118 of 12 January 2021; Governo Federal do Brazil: Brasília, Brazil, 2021.
31. Malta, N.S.; Rabbi, I.M.; Rodrigues, E.A.N. Conforto térmico, eficiência energética e viabilidade econômica em HIS. *PARC Pesqui. Em Arquitetura Construção* **2022**, *13*, e022020. [CrossRef]
32. Dalbem, R.; Cunha, E.G.; Vicente, R.; Figueiredo, A.; Oliveira, R.; Silva, A.C.S.B. Optimisation of a social housing for south of Brazil: From basic performance standard to passive house concept. *Energy* **2019**, *167*, 1278–1296. [CrossRef]
33. *NBR 15220*; Thermal Performance of Buildings. ABNT–Brazilian Association of Technical Standards: Rio de Janeiro, Brazil, 2024.
34. Vaz, J. Experimental and Numerical Study on the Use of Soil as an Energy Reservoir for Heating and Cooling of Built Environments in Southern Brazil. Ph.D. Thesis, Federal University of Rio Grande do Sul (UFRGS), Porto Alegre, Brazil, 2011.
35. Vaz, J.; Sattler, M.A.; Dos Santos, E.D.; Isoldi, L.A. Experimental and Numerical Analysis of an Earth–Air Heat Exchanger. *Energy Build.* **2011**, *43*, 2476–2482. [CrossRef]
36. Rodrigues, M.K.; Brum, R.S.; Vaz, J.; Rocha, L.A.O.; Santos, E.D.; Isoldi, L.A. Numerical investigation about the improvement of the thermal potential of an Earth-Air Heat Exchanger (EAHE) employing the Constructal Design method. *Renew. Energy* **2015**, *80*, 538–551. [CrossRef]
37. Moura, P.W.; Leite, L.R.; Moura, M.W.; Rocha, L.A.O.; Santos, E.D.; Brum, R.S.; Isoldi, L.A. Numerical Evaluation of the Influence of Different Parameters on the Thermoenergetic Performance of the Earth-Air Heat Exchanger in a Social Housing. *Defect Diffus. Forum* **2024**, *436*, 17–126. [CrossRef]
38. CAIXA. *Housing—Minha Casa, Minha Vida*; Standard Project: Social Housing; CAIXA Notebooks; CAIXA: Brasília, Brazil, 2009. Available online: https://www.caixa.gov.br/site/paginas/downloads.aspx (accessed on 30 August 2021).
39. Governo Federal do Brazil. *Provides Guidelines for the Preparation of Projects and Establishes the Minimum Technical Specifications for Housing Units and the Urban Planning Specifications of Developments Intended for Acquisition and Transfer Using Resources Derived from the Capitalization of Shares in the Residential Leasing Fund (FAR), as Well as for the Contracting of Operations with Resources Transferred to the Social Development Fund (FDS), Within the Scope of the Minha Casa, Minha Vida Program (PMCMV)*; Ordinance No. 660 of 14 November 2018; Governo Federal do Brazil: Brasília, Brazil, 2018.
40. *NBR 15575*; Residential Buildings—Performance. ABNT–Brazilian Association of Technical Standards: Rio de Janeiro, Brazil, 2021.
41. Oke, T.R. *Boundary Layer Climates*; Routledge: London, UK, 2002.
42. DOE-Department of Energy Efficiency and Renewable Energy. *Engineering Reference. EnergyPlus. Version 9.4.0, Documentation*; DOE: Washington, DC, USA, 2022.
43. Alves, A.B.M.; Schmid, A.L. Cooling and heating potential of underground soil according to depth and soil surface treatment in the Brazilian climatic regions. *Energy Build.* **2015**, *90*, 41–50. [CrossRef]
44. Lamberts, R.; Dutra, L.; Pereira, F.O.R. *Energy Efficiency in Architecture*, 3rd ed.; LABEEE: Florianópolis, Brazil, 2014. Available online: https://labeee.ufsc.br/pt-br/publicacoes/livros (accessed on 8 November 2025).
45. Zhao, J.; Huang, B.; Li, Y.; Zhao, Y. Comprehensive Review on Climatic Feasibility and Economic Benefits of Earth-to-Air Heat Exchanger (EAHE) Systems. *Sustain. Energy Technol. Assess.* **2024**, *68*, 103862. [CrossRef]
46. Brazil Escola. Map of the climates of Brazil. In *The Climates of Brazil*; Brazil Escola: Goiânia, Brazil, 2025. Available online: https://brasilescola.uol.com.br/brasil/os-climas-brasil.htm (accessed on 18 May 2026).